Spectrochimica Acta Part A: Molecular and Biomolecular Spectroscopy 226 (2020) 117553

Contents lists available at ScienceDirect

Spectrochimica Acta Part A: Molecular and Biomolecular Spectroscopy

journal homepage: www.elsevier.com/locate/saa

Interaction of aromatic compounds and anions with naphthylimide-dansylamide fluorescent dyad: Experimental evidence of aryl C—H…π and aryl C—H…anion contacts and DFT calculations

Miguel Ángel Claudio-Catalán [a], Felipe Medrano [b], Hugo Tlahuext [c], Nadia Alejandra Rodríguez-Uribe [c], Carolina Godoy-Alcántar [c, *]

[a] Departamento de Ciencias Químico-Biológicas, Instituto de Ciencias Biomédicas, Universidad Autónoma de Ciudad Juárez, Avenida Plutarco Elías Calles, 1210, Fovissste Chamizal, Ciudad Juárez, Chihuahua, Mexico
[b] Departamento de Ciencias Químico-Biológicas, Universidad de Sonora, Rosales y Luis Encinas s/n, Hermosillo, Sonora, 83000, Mexico
[c] Centro de Investigaciones Químicas, IICBA, Universidad Autónoma del Estado de Morelos, Av. Universidad 1001, Col. Chamilpa, Cuernavaca, Morelos, 62209, Mexico

ARTICLE INFO

Article history:
Received 9 July 2019
Received in revised form
2 September 2019
Accepted 18 September 2019
Available online 10 October 2019

Keywords:
Aryl C—H…anion
Aryl C—H…π
Naphthylimide-dansylamide
Dyad
Density functional theory

ABSTRACT

In this work the interaction of halide anions and simple aromatic compounds with a bichromophoric fluorescent dyad derived from 1,8-naphthalimide (NAPIM) and 5-(dimethylamino)naphthalene-1-sulfonyl (DANS) was studied using electronic spectroscopy, ^{1}H, and ^{19}F NMR spectroscopy and quantum chemistry modeling (b3lyp/def2-TZVP). The NAPIM-DANS dyad interacts with electron-rich guests with binding constants in the range of 6×10^{3} to 8×10^{3} M^{-1} in $CHCl_3$. The formed complexes are stabilized through aryl C—H … anion and aryl C—H … π interactions.

1. Introduction

Recently, some research groups have reported the synthesis of fluorescent dyads containing 5-(dimethylamino)naphthalene-1-sulfonyl (dansyl, DANS) and 1,8-naphthalimide (NAPIM) fluorophores due to the excellent photophysical properties of the aromatic groups present in its structure [1–3]. Thus, Li and coworkers have reported the use of a NAPIM fluorescent dyad as a probe for imaging the nitric oxide (NO) distribution in the endoplasmic reticulum [4].

According to Pischel and coworkers [1], the interesting feature of these bichromophoric systems is the presence of two competing relaxation processes: photoinduced electron transfer (PET) from dansyl to the naphthalimide moiety and singlet-singlet energy-transfer (SSET) from the naphthalimide to the dansyl entity. The estimated rates of the PET and SSET indicate that both these relaxation processes decrease with the increase in the length of the spacer group.

Also, chromophoric and fluorescent sensors has been made with dyads that combine NAPIM units with metal binding aromatic groups. As an example, some reports demonstrate that these kind of compounds can interact selectively with Cu^{2+} over other divalent metal ions. In this case, the binding event was signaled through the inhibition of intramolecular fluorescence resonance energy transfer (FRET)-mediated emission [3,5].

On the other hand, our quantum chemistry calculations of the electrostatic potential of this kind of compounds showed that both NAPIM and DANS aromatic rings are electron deficient which is adequate to form host-guest complexes with anions and aromatic compounds *i.e.*, electron-rich molecules. To the best of our knowledge there is only one work in the literature about the interaction of bis-NAPIM dyad with fluoride anion, but in that work, the process of sensing is the irreversible deprotonation of one amino group induced by fluoride in acetonitrile [6].

Recently, we reported the crystal structure of bis-(DANS)-NAPIM compound (*N,N′*-bis[2-((benzyl){[5-(dimethylamino)naphthalen-1-yl]sulfonyl}amino)ethyl]naphthalene-1,8:4,5-tetracarboximide) in which two DANS aromatic rings stack around the NAPIM moiety forming a sandwich arrangement [7].

* Corresponding author.
E-mail address: cga@uaem.mx (C. Godoy-Alcántar).

https://doi.org/10.1016/j.saa.2019.117553
1386-1425/

In this work, we studied by spectroscopic methods the interaction of the DANS-NAPIM dyad **2** with electron rich species as halide anions (F^- and Br^- as TBA salts) and neutral aromatic compounds (benzene and naphthalene) in chloroform. Also, ^1H NMR titration experiments and molecular modeling studies at DFT theory level supported that weak aryl C—H … anion and aryl C—H … π interactions stabilize the structure of the complexes formed between dyad **2** with the studied guests.

2. Experimental section

2.1. Materials and equipment

All reagents and solvents were acquired from the Aldrich Chemical Company and were used without further purification. ^1H and ^{13}C NMR spectra were recorded at room temperature with a Varian VXR 400 MHz spectrometer. Tetramethylsilane for ^1H (TMS, internal, δ = 0.00 ppm), chloroform for ^{13}C (δ = 77.23 ppm), tetrahydrofuran-d8 ^1H (δ = CH_2 (2,5) 3.58 ppm, CH_2 (3,4) 1.72 ppm) and KF in D_2O (1.5 M) for ^{19}F (δ = −121.7 ppm) were used as standard references. 2D COSY and heteronuclear correlation (HETCOR) experiments were performed for the unambiguous assignment of the ^1H and ^{13}C NMR spectra. IR spectra were recorded on a Nicolet 6700 FT-IR Thermo Scientific spectrophotometer. Mass spectra were obtained with a Jeol JMS 700 MStation instrument. Melting points were determined with a Büchi B-540 digital apparatus. The electronic absorption spectra were recorded at 25 °C on a Hewlett—Packard 8452A diode array spectrophotometer. The excitation and emission fluorescence spectra were recorded at 25 °C on a PerkinElmer luminescence spectrometer model LS55. Conductometry was performed with YSI 3200 conductivity meter.

2.2. Synthesis of naphthalimide-dansylamide dyad

Compound 1. To a solution of 1,8-naphthalic anhydride (0.5 g, 2.52 mmol) in 25 mL of toluene 0.45 mL (0.455 g, 3.03 mmol) of *N*-benzylethylendiamine were added followed by the addition of triethylamine (0.255 g, 2.52 mmol). The reaction mixture was heated to reflux under azeotropic removal of water with a Dean-Stark trap for 22 h. The solution was cooled, and the solvent was removed under reduced pressure. The resultant oil was purified by column chromatography on silica gel (CH_2Cl_2—MeOH 98:02). The compound **1** was obtained as a white powder (0.718 g, 86%). M.p. 110—111 °C. FTIR (neat): 2836, 1698, 1655, 1625 cm^{-1}. ^1H NMR (400 MHz, $CDCl_3$) δ: 1.81 (s, 1H, NH), 3.02 (t, J = 6.4 Hz, 2H, CH_2NH), 3.85 (s, 2H, CH_2Ph), 4.36 (t, J = 6.4 Hz, 2H, NCH_2), 7.16—7.20 (m, 1H, $H_{aromatic}$), 7.22—7.31 (m, 4H, $H_{aromatic}$), 7.72 (t, J = 8.0 Hz, 2H, $H_{aromatic}$), 8.17 (d, J = 8.8 Hz, 2H, $H_{aromatic}$), 8.56 (d, J = 7.6 Hz, 2H, $H_{aromatic}$). ^{13}C NMR (100 MHz, $CDCl_3$) δ: 40.0 (NCH_2), 47.1 (CH_2NH), 53.6 (CH_2Ph), 122.7, 126.9, 127.0 (2C), 127.1, 128.2 (2C), 128.4 (2C), 131.3 (2C), 131.6, 134.0 (2C), 140.3, 164.5 (C=O). MS (FAB^+): *m/z* (%) 331 (100) $[M + H]^+$; HRMS (FAB^+): calculated for $C_{21}H_{19}O_2N_2$ $[M + H]^+$, *m/z* 331.1447; found for $[M + H]^+$, *m/z* 331.1461.

Dyad 2. A mixture of imide **1** (0.2 g, 0.605 mmol), dansyl chloride (0.163 g, 0.605 mmol) and K_2CO_3 (0.084 g, 0.605 mmol) in chloroform/water (4:1) (10 mL) was stirred at room temperature for 12 h. The organic layer was extracted with dichloromethane (2 × 20 mL), dried over anhydrous Na_2SO_4, filtered and concentrated under reduced pressure. Further purification was performed by flash chromatography on silica gel (CH_2Cl_2—MeOH 98:02). The compound **2** was obtained as a yellow solid (0.317 g, 93%). The crystallization from a chloroform-toluene mixture afforded suitable crystals for X-ray crystallographic analysis. M.p. 174—175 °C. FTIR (neat): 1698, 1660, 1587, 1320, 1138 cm^{-1}. ^1H NMR (400 MHz, $CDCl_3$) δ: 2.65 (s, 6H, $(CH_3)_2N$), 3.65 (t, J = 6.0 Hz, 2H, CH_2NSO_2), 4.20 (t, J = 6.0 Hz, 2H, CH_2NCO), 4.97 (s, 2H, CH_2Ph), 6.63 (d, J = 7.2 Hz, 1H, $H_{aromatic}$), 7.17 (dd, J = 8.4, 7.6 Hz, 1H, $H_{aromatic}$), 7.23—7.32 (m, 4H, $H_{aromatic}$), 7.37—7.40 (m, 2H, $H_{aromatic}$), 7.65 (t, J = 8.0 Hz, 2H, $H_{aromatic}$), 7.97 (t, J = 8.4 Hz, 2H, $H_{aromatic}$), 8.11 (dd, J = 8.4, 1.2 Hz, 2H, $H_{aromatic}$), 8.16 (dd, J = 7.2, 1.2 Hz, 1H, $H_{aromatic}$), 8.31 (dd, J = 7.2, 1.2 Hz, 2H, $H_{aromatic}$). ^{13}C NMR (100 MHz, $CDCl_3$) δ: 37.0 (CH_2NCO), 42.9 (CH_2NSO_2), 45.3 (2C, $(CH_3)_2N$), 49.5 (CH_2Ph), 114.1, 118.9, 122.2, 122.9, 126.7 (2C), 127.9, 128.1, 128.8 (2C), 129.1 (2C), 129.2, 129.6, 130.1, 130.7, 131.2 (2C), 131.4, 133.8 (2C), 134.7, 135.9, 151.1, 164.0 (C=O). MS (FAB^+): *m/z* (%) 564 (70) $[M + H]^+$; HRMS (FAB^+): calculated for $C_{33}H_{30}O_4N_3S$ $[M + H]^+$, *m/z* 564.1952; found for $[M + H]^+$, *m/z* 564.1878.

2.3. X-ray crystallography

Single-crystal X-ray diffraction studies were performed on a SuperNova, Dual, Cu at zero, EosS2 diffractometer ($\lambda Cu_{K\alpha}$ = 1.54184 Å, monochromator: mirror). The crystal was kept at 295.41(10) K during data collection. Using Olex2 [8], the structure was solved with the ShelXT structure solution program using Direct Methods and refined with the ShelXL refinement package using Least Squares minimisation [9].

Non-hydrogen atoms were refined anisotropically, while hydrogen atoms were placed in geometrically calculated positions using a riding model. DIAMOND [10] was used for the creation of Fig. 2, Crystallographic data for the structure of dyad **2** reported in this paper have been deposited with the Cambridge Crystallographic Data Centre as supplementary publications no. CCDC 1481978. Copies of the data can be obtained free of charge on application to CCDC, 12 Union Road, Cambridge CB2 1EZ, UK (fax: (+44)1223-336-033; e-mail: deposit@ccdc.cam.ac.uk, www: http://www.ccdc.cam.ac.uk).

2.4. UV/vis titrations

The spectrometric titrations were performed at 25 °C in chloroform. Aliquots of 1×10^{-2} M solution of the guest were added to the dyad **2** solution 8×10^{-5} M. The spectra were recorded after each addition. The spectral changes were corrected by dilution effect and by the absorbance of the guest thus the absorbance corrected was plotted versus the guest concentration for fitting the experimental points and calculate the binding constants. The experimental data were fitted using non-linear least-squares regression with Microcal Origin 5 program.

2.5. Fluorescence spectra

The emission (λ_{exc} = 337 nm) and excitation (λ_{em} = 381 nm) spectra of the dyad **2** was recorded at 1×10^{-5} M at 298.15 K in $CHCl_3$. Aliquots of guest 1×10^{-2} M were added to dyad solution to obtain the stoichiometries 1:1 and 1:2 dyad **2**:guest then emission spectra were recorded at each stoichiometry ratio.

2.6. ^1H NMR titrations

^1H NMR titration experiments were performed in $CDCl_3$ solution by adding aliquots of a concentrated guest stock solutions to a 4.4×10^{-2} M solution of dyad **2** to obtain 1:1 and 1:2 dyad **2**:guest stoichiometric relationships. The same procedure was used for the titration of dyad **2** with TBA^+F^- in THF-d8.

2.7. Computational details

The molecular structure of complexes was calculated by computational chemistry methods at density functional theory (DFT) using the well-known Becke— Lee—Yang—Parr three parameters (B3LYP) hybrid functional [11] with Aldrichs def2-TZVP basis

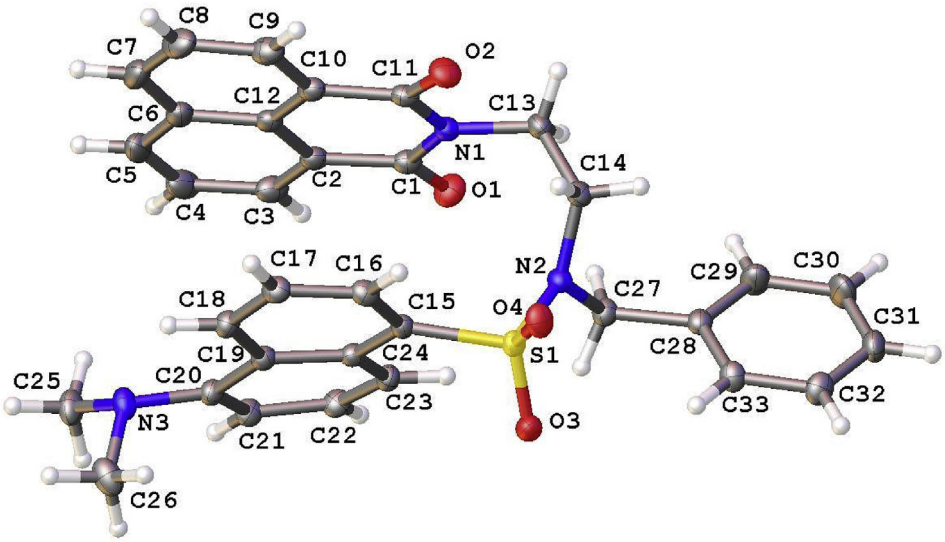

Fig. 1. X-ray molecular structure of dyad **2** showing the atom-labeling according to Scheme 1. Displacement ellipsoids are drawn at the 50% probability level and H atoms are shown as small spheres of arbitrary radius.

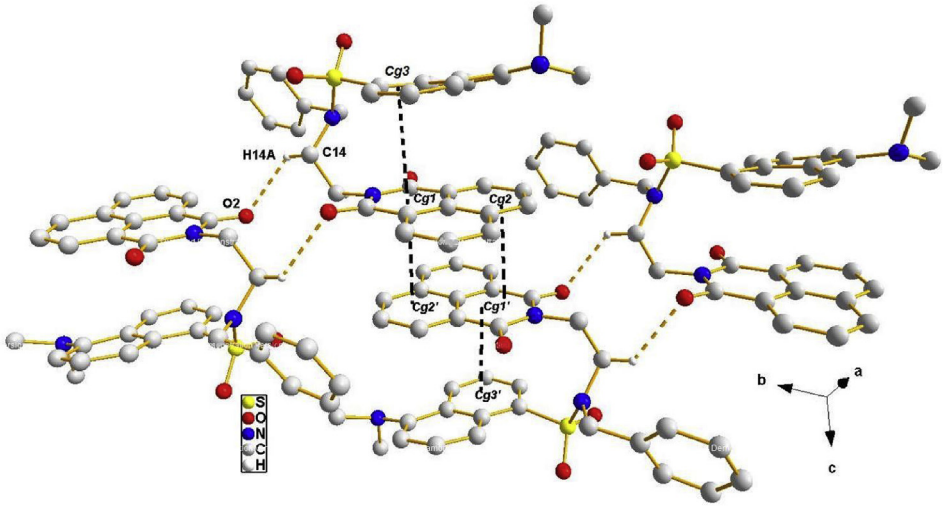

Fig. 2. A view of the crystal packing of dyad **2**, showing C—H···O and π ... π contacts (dashed lines). Hydrogen atoms not involved in the hydrogen bonds have been omitted for clarity.

set as implemented in Gaussian [12]. Electronic transitions for dyad **2** were calculated by TD-DFT (B3LYP/6-311 + G**). All the calculations were done in chloroform using Tomassi PCM [13] with the integral equation formalism variant (IEFPCM) in which the solute cavity is created via a set of overlapping spheres.

3. Results and discussion

3.1. Characterization

3.1.1. Crystal structure of dyad *2*

Dyad **2** was prepared in 86% yield according to Scheme 1. A single crystal of dyad **2** could be grown at room temperature by slow evaporation of chloroform-toluene mixture. Fig. 1 shows the X-ray molecular structure of dyad **2**. The most relevant crystallographic data are summarized in Table S1 (Supplementary Material).

In the molecular structure of dyad **2,** the bond distances and angles have normal values. The fragments 1,8-naphthalimide (N1/C1/C2/C12/C10/C11) and phenyl (C28—C33), are almost planar with r.m.s. deviations of 0.025, 0.001 Å, respectively. In the dansyl group, the rings (C15—C19/C24) and (C19—C24) have r.m.s. deviations of 0.032 and 0.028 Å with an interplanar angle of 7.715(0.077)°. The torsion angle N1—C13—C14—N2 is 61.97(14)°. This conformation is stabilized by an offset π-π interaction between the adjacent aromatic rings, with a distance between the ring centroids Cg1 and Cg3 (Cg1 is the centroid of N1/C1/C2//C12/C10/C11 and Cg3 is the centroid of the ring C15—C19/C24) of 3.5995(1) Å. Also, C—H···O and C—H···N intramolecular hydrogen bonds were detected (Table S2) [14].

The crystal packing is stabilized by offset π-π stacking between two adjacent molecules with a distance between the ring centroids Cg1 and Cg2' (Cg1 is the centroid of the ring N1/C1/C2/C12/C10/C11 and Cg2' is the centroid of the ring C2—C6/C12; (*i*) symmetry operator: 1-x, 1-y, 1-z) of 3.5547(1) Å, generating centrosymmetric motifs which are interconnected through C—H···O hydrogen bonds (Fig. 2).

3.1.2. UV/vis spectrum of dyad *2*

The solution spectrum of the dyad **2** in $CHCl_3$ (Fig. S1) has three π—π* transition bands in the near UV spectral region. The 259 nm

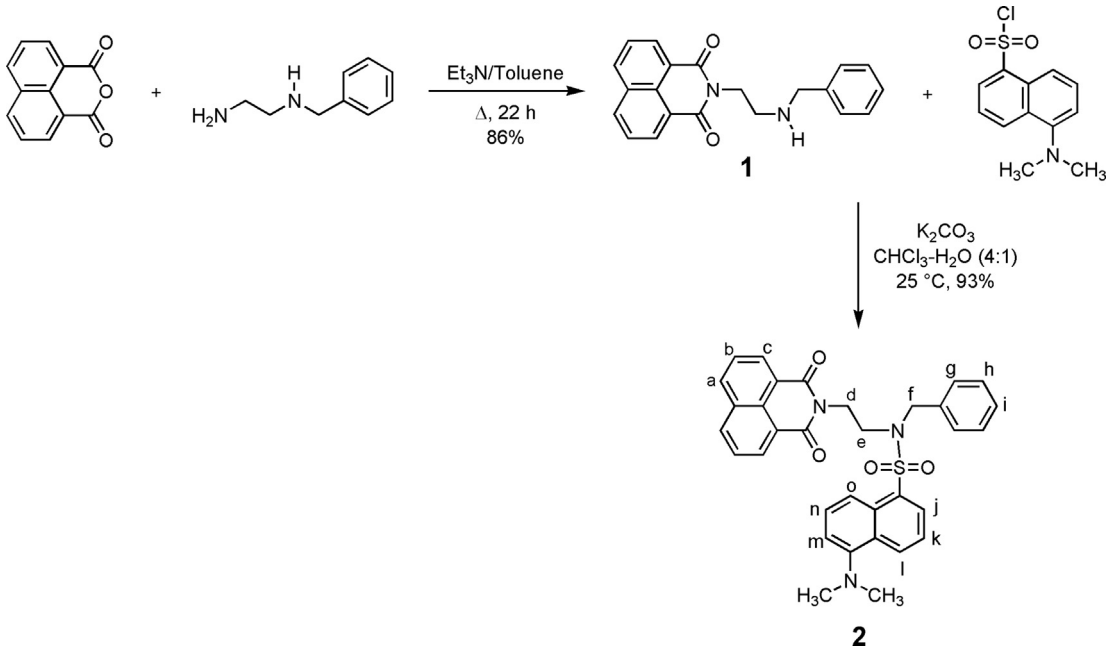

Scheme 1. Synthetic route for the preparation of dyad **2**.

(ε = 13523 ± 508 $M^{-1}cm^{-1}$) band was observed as an ill-defined shoulder on a strong absorption envelope at the shorter wavelength side. In the region of 300–380 nm two partially overlapped bands with maxima located at 336 nm ($\varepsilon = 16168 \pm 526\ M^{-1}cm^{-1}$) and 350 nm ($\varepsilon = 13211 \pm 309\ M^{-1}cm^{-1}$) were observed. The last band has a slightly lower intensity. Both bands were assigned to the aromatic imide moiety as the reported UV–vis spectrum *n*-butyl naphthalene imide [15] showed two strong bands at 331 nm ($\varepsilon = 1.18 \times 10^4\ M^{-1}cm^{-1}$) and 341 nm ($\varepsilon = 1.41 \times 10^4\ M^{-1}cm^{-1}$). On the other hand, the dansyl absorption bands are in the same spectral region [16], $\lambda = 340$ nm ($\varepsilon = 4 \times 10^3\ M^{-1}cm^{-1}$) but with a lower intensity, so they are overlapped with the NAPIM bands.

3.1.3. Fluorescence spectra of dyad **2**

The emission spectrum of dyad **2** consists of two bands centered at $\lambda = 381$ nm and $\lambda = 483$ nm. On the other hand, the excitation spectrum showed a long wavelength maximum at $\lambda = 337$ nm, Fig. S2. Comparing the observed data with the reported spectra for other DANS-NAPIM dyads [2,16], the $\lambda = 381$ nm emission band correspond to NAPIM aromatic ring while the $\lambda = 483$ nm correspond to the DANS moiety [2].

Theoretical calculations at time domain density functional theory (TD-DFT) were performed to know the origin and nature of the electronic transitions observed in the electronic spectra. TD-DFT/B3LYP/6-311 + G(d) theory level calculations showed that the 336 nm band is associated to the electronic transition from HOMO-1 to LUMO, while the 350 nm band was ascribed to the electronic jump from HOMO to LUMO+1. Both HOMO-1 and HOMO levels are molecular orbitals with electronic density located over the dansyl moiety. On the other hand, LUMO and LUMO+1 energy levels have electronic density centered over the naphthylimide moiety. The Fig. S3 shows the molecular orbitals involved in the transitions. These findings suggest that charge is transferred between the dansyl sulfonamide chromophore to the naphthylimide moiety. This finding agrees with the experimental data published by Pischel and coworkers [1] who reported the photophysical properties of NAPIM-DANS dyads in acetonitrile. For 5-(dimethylamino)-N-(2-(1,3-dioxo-1H-benzo[de]isoquinolin-2(3H)-yl) ethyl)naphthalene-1-sulfonamide which is a dyad **2** analog, the DANS fluorescence is quenched (emission efficiency $\leq 0.2\%$) with respect to a model compound 4-(dimethylamino)-N-ethylnaphthalene-1-sulfonamide ($\varphi_f = 0.30$). In this case, the quenching mechanism is through a fast singlet-singlet energy transfer (SSET) which is assumed to proceed via a Coulombic mechanism which was corroborated by the large spectral overlap integral ($J_{Coulombic} = 3.1 \times 10^{-12}\ cm^6\ mol^{-1}$).

3.2. Molecular recognition experiments

From X-ray structure of dyad **2** we observed a stacked arrangement for DANS and NAPIM moieties. Additionally, the spacer group that binds the aromatic rings in dyad **2** is short enough to bring the chromophores to close together, which can impart novel photophysical properties during the recognition event considering their electron deficient nature.

3.2.1. Measurement of association constants by UV/Vis spectroscopy

The ability of dyad **2** to bind aromatic and anion guests according to Equation (1) was tested by UV/Vis titrations. The addition of aliquots of a concentrated solution of the guest induces a small hyperchromic shift in absorption bands of the recorded spectrum (Fig. S4).

The absorption recorded at different wavelengths were plotted versus the guest concentration (Fig. S5) and analyzed using an equation which assumes a 1:1 complex with a ratio [guest] » [dyad **2**] to calculate the binding constants [17].

$$H + G \leftrightarrow HG \tag{1}$$

The measured binding constants are presented in Table 1. These data show that dyad **2** can bind aromatic and anionic guests with association constants in the range of ~10^3- $10^4\ M^{-1}$ and preferring the smaller guests such as benzene and F^- than the larger guests as naphthalene and Br^-.

3.2.2. Interactions observed on emission spectra

To observe the effect of the studied substrates on the emission spectra of dyad **2,** aliquots of the benzene or fluoride were added to

Table 1
Binding constants of dyad **2** to neutral and anionic guests in $CHCl_3$ at 25 °C obtained by spectrophotometric titrations.

Guest	K (M^{-1})
Benzene	8751 ± 890
Naphtalene	6093 ± 908
F^- [a]	7397 ± 720
Br^- [a]	6160 ± 1036

[a] As tetrabutylammonium salts.

receptor solutions to obtain mixtures with 1:1 stoichiometry and their fluorescence spectra were recorded (Fig. 3). As can be observed only the band assigned to naphthylimide presents changes, *i.e.,* for the complex dyad **2**-benzene the intensity of emission band is enhanced while for dyad **2**-F^- complex the fluorescence is quenched (decreased). These findings suggest that

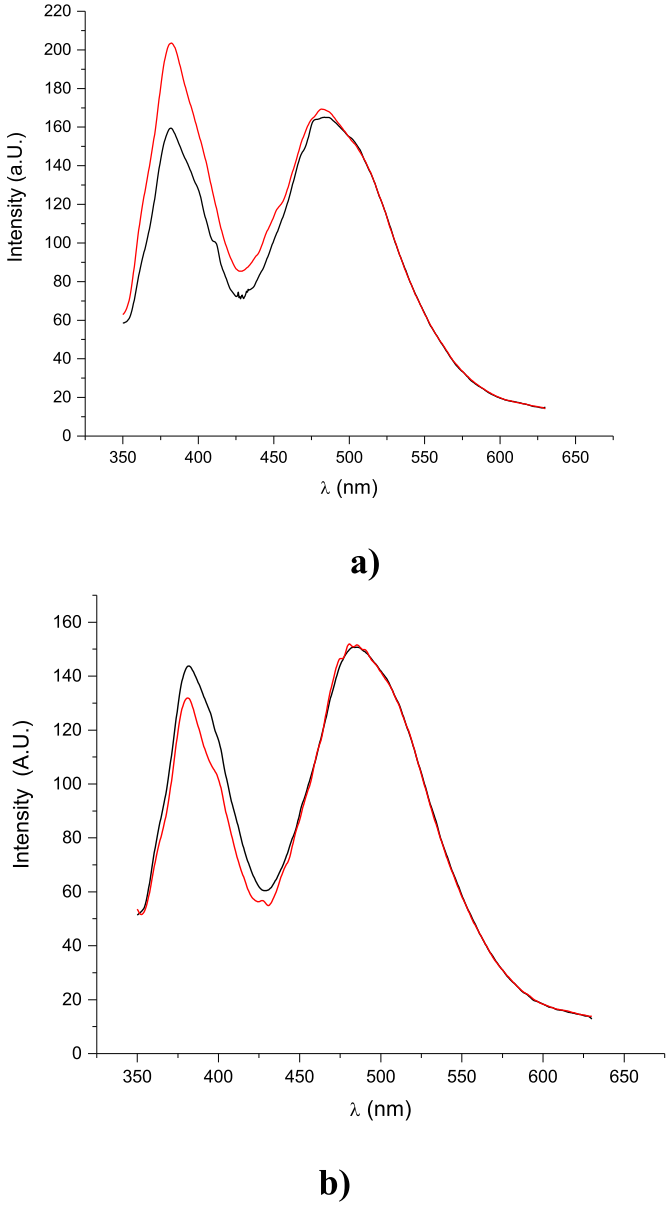

Fig. 3. Emission spectra of dyad **2** (black line) at 1×10^{-5} M in $CHCl_3$, 25 °C with $\lambda_{exc} = 337$ nm and emission spectra of dyad **2** after one equivalent of a) benzene and b) TBA^+F^-, both showed in red line.

NAPIM aromatic moiety is involved in the interaction with the guests. It is interesting to observe that dyad **2** can act as ON/OFF sensor depending on the nature of the complexed guest. Aromatic compounds enhance the fluorescence emission by donating electronic density towards dyad **2**, while anionic guests quench the emission by extracting electronic density from dyad **2** chromophores.

Naphthalene and Br^- induced slightly changes on fluorescence spectra of dyad **2** (Fig. S6), suggesting that the size and nature of the involved guest are important factors for the complex formation.

3.2.3. Interactions observed on NMR titrations

^1H NMR spectrum of dyad **2** in $CDCl_3$ has been completely assigned (see experimental section for chemical shifts and labels of protons in Scheme 1).^1H and ^{19}F NMR titration experiments were carried out to obtain structural information about the interaction sites of the dyad **2** with the guests. In these experiments, small volumes of a concentrated solution of the studied guest were added to a receptor solution until different molar ratios were achieved.

In the titration of dyad **2** with benzene (Fig. S7), the addition of one equivalent of the guest to dyad **2** solution causes a broadening of all aromatic signals while the signals corresponding to the methylene (H_d, H_e, H_f) and methyl ($N(CH_3)_2$) protons are not affected The broadening of the signals is consistent with aryl C—H .. π interaction as has been observed for other aromatic receptors based on naphthalene imides [18]. On the other hand, Fig. S8 shows the titration of dyad **2** with naphthalene. As can be see it, the addition of up to two equivalents of naphthalene produce a slight broadening of the all proton signals suggesting the complex formation through aryl C—H … π interactions, which are supported by the results of DFT theoretical calculations (*vide infra*). The C—H atoms located close to the face of the aromatic moiety suffer an upfield shift due to protecting effect of the ring current as has been observed in other systems [19].

Fig. S9 and Fig. S10 show the titrations of dyad **2** with the anionic guests TBA^+F^- and TBA^+Br^-, respectively. In both cases, the changes observed can be explained by the establishment of aryl C—H … X (X = F^-or Br^-) interactions.

Additional evidence of the complex formation was obtained from a^{19}F NMR titration. In this experiment, a solution of TBA^+F^- was titrated with a solution of dyad **2**. Fig. 4a shows the spectra of free TBA^+F^- which consist in a fine signal centered at −131.4 ppm. Upon the addition of one equivalent of dyad **2**, the spectrum is transformed in a broad signal (−126.6 ppm). The down field shift (~5 ppm) of ^{19}F signal can be attributed to the density loss of the F^- anion by interaction with an aromatic ring through aryl C—H···F^- contact.

It is important to consider that in low polarity solvents, as chloroform, the ionic salts are dissolved as ion-pairs. The presence of such species has a deep effect on the measurement of association constants by techniques that employ high ionic salt concentrations, as is the case of NMR. Fortunately, the measurement of the electrical conductivity of the solution is an experimental technique sensitive to the degree of dissociation of ionic salts in organic solvents, hence, we carried out a conductimetric titrations of a solution of TBA^+F^- (1×10^{-4} M) with dyad **2** in $CHCl_3$ (ε = 4.8). A plot of conductivity *vs* [dyad **2**]/[TBA^+F^-] molar ratio (Fig. S11) showed that under these experimental conditions the presence of the dyad **2** has no significant effect on the conductivity of the TBA^+F^- solution and indicates that the interaction of the receptor is with the TBA^+F^- ion-pair.

As the polarity of the solvent has a strong effect on the degree of dissociation of an ionic salt, we carried out a similar conductimetric titration but using THF (ε = 7.6) as solvent. In this case, the addition of the dyad **2** to the TBA^+F^- solution caused a notorious increase in the conductivity due the transformation of ion pair to free ions

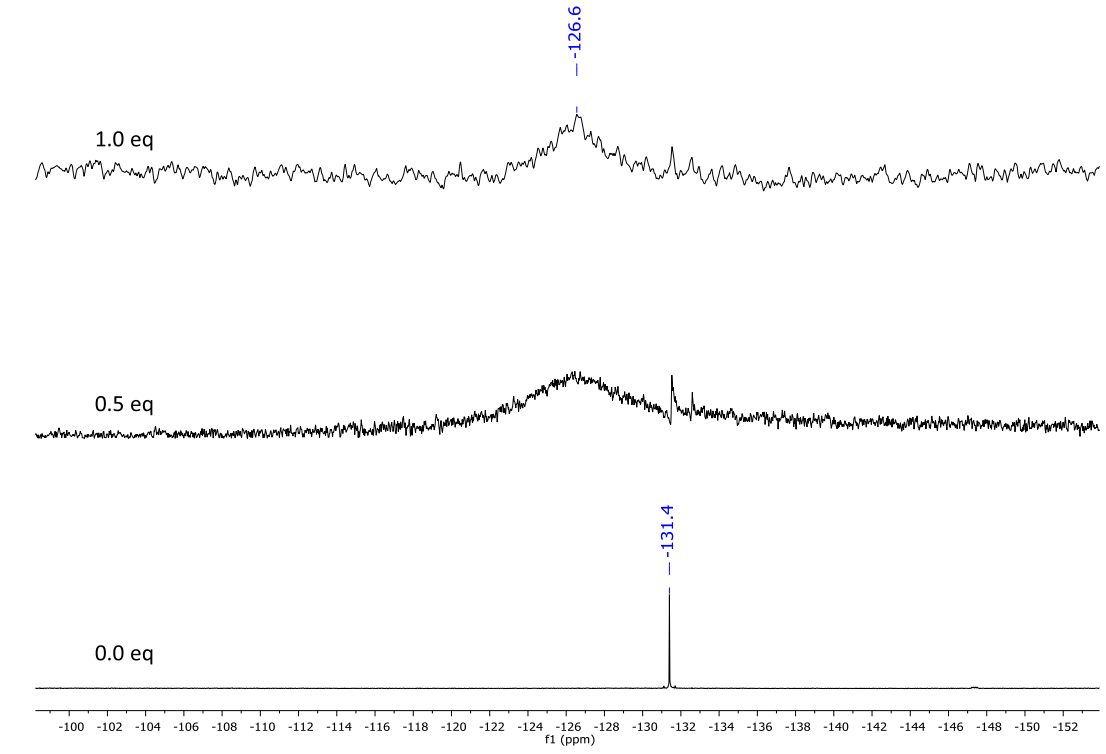

a

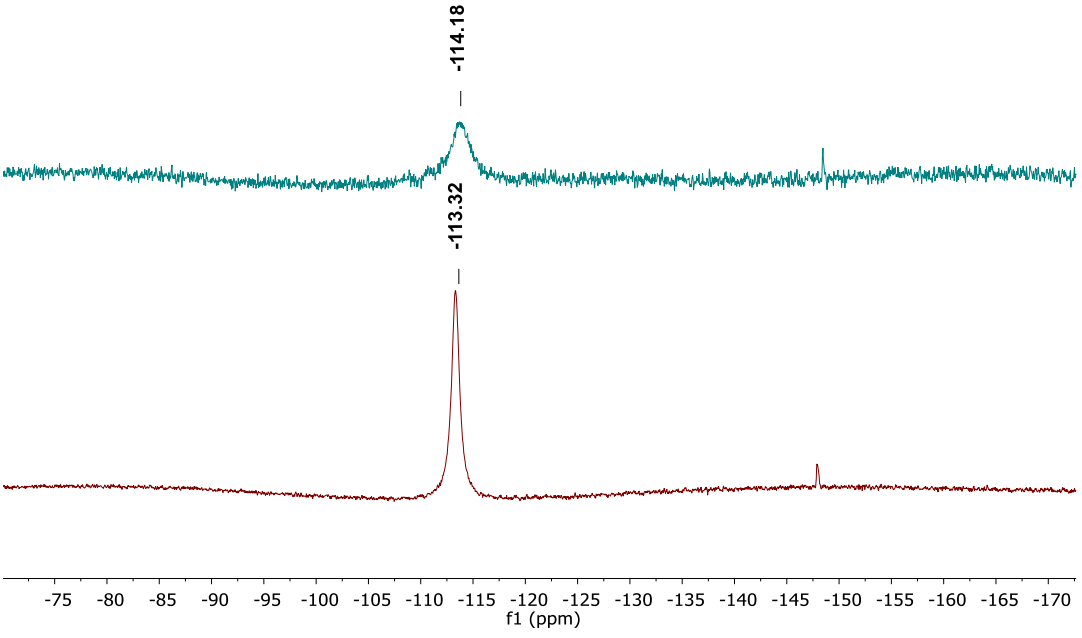

b

Fig. 4. ^{19}F NMR 188.1 MHz of $TBA^{+}F^{-}$ (4.4×10^{-2} M) in a) $CDCl_3$ with different equivalents of dyad **2,** b) THF- d8 with zero (red) and two equivalents (blue) of dyad **2.**

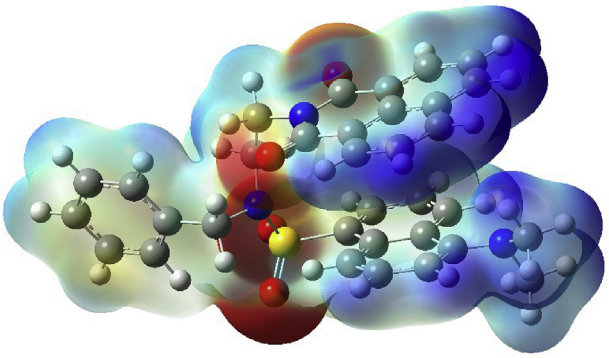

Fig. 5. Electrostatic surface potentials calculated for dyad **2** using b3lyp/6-31G(**) level of theory. The relatively high electron density is shown in red and the shortage of electron density is shown in blue.

(Fig. S11). These phenomenon has been observed by Sada and co-workers who investigated the interaction of anions with calix [4] pyroles in organic solvents [20].

In order to obtain structural information of the complex dyad **2**–TBA^+F^- in THF- d8 we carried out ^1H and ^{19}F NMR experiments. As we can observe on the ^1H spectrum (Fig. S12) the signals of protons H_c and H_j are broadening in higher degree than in the case of $CDCl_3$ solvent (Fig. S9) while in the ^{19}F spectrum we observed a broadening of the signal of F^- once formed the complex with dyad **2** without change in its chemical shift (Fig. 4b). Comparing the ^{19}F spectra of TBA^+F^- in both solvents $CDCl_3$ and THF-d8 (Fig. 4) we observe a fine signal in $CDCl_3$ case and slightly broadening in THF-d8, probably due to no-dissociate condition in the first solvent and an equilibrium between TBA^+F^- ion pair and the dissociated F^- anion. In the dyad **2** + TBA^+F^- mixture in $CDCl_3$, we observe a ternary complex formed between dyad **2** and the ion pair (*vide infra*). On the other hand, while in the THF- d8 solutions an equilibrium between dyad **2**-F^- and dyad **2**–TBA^+F^- species could be established as was discussed by Sada and coworkers [20].

3.3. Quantum chemistry structural studies

We carried out computational chemistry calculations at the DFT level of theory to establish a probable structure of the complexes. The initial structure of the dyad **2** was that obtained by X-ray diffraction analysis, while the guests were located according to the information provided by the NMR experiments. First, is important to mention that the electrostatic potential calculated for dyad **2** (Fig. 5) show significant polarization due the electron-withdrawing carbonyl and sulfonyl substituents attached to the aromatic moieties. Both NAPIM and DANS aromatic units are electron deficient, while benzene, naphthalene, and the halide anions are relatively electron rich. From this analysis, we conclude that interactions

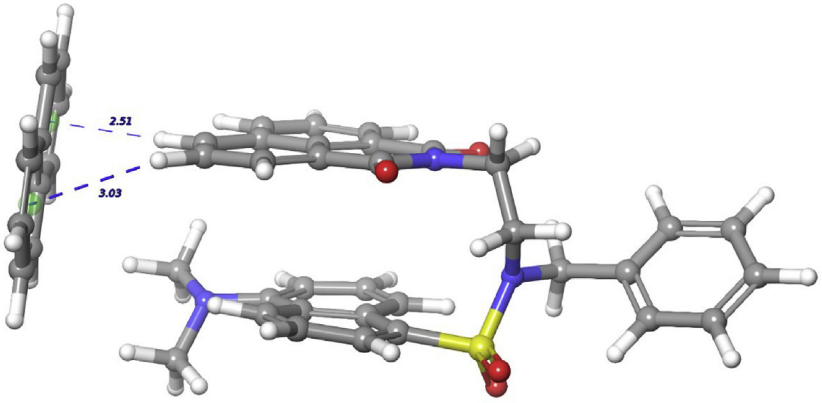

a)

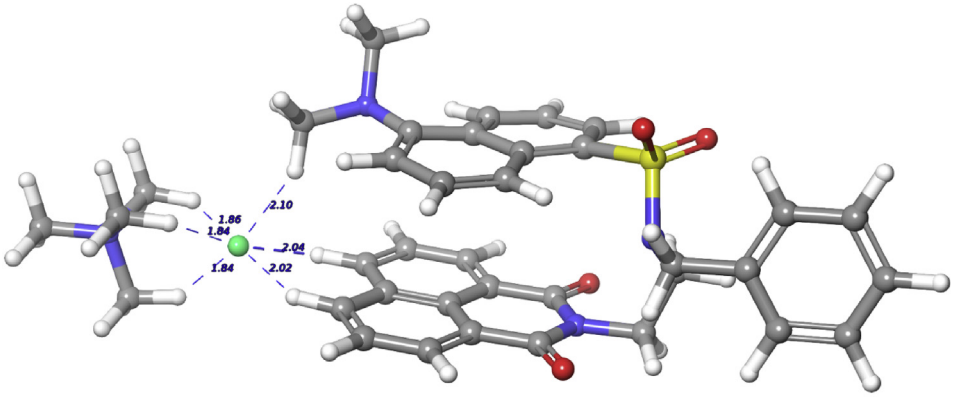

b)

Fig. 6. Geometry optimized structures for the complexes in chloroform: a) dyad **2**-naphthalene and b) dyad **2**-TBA^+F^-. The calculations were done with DFT (B3LYP/def2-TZVP) and polarizable continuum (PCM-IEFPCM) to model the solvent.

between these complementary electrostatic surfaces could provide a significant driving force for host-guest complex formation.

Fig. 6 shows the optimized structures of the complexes with naphthalene and fluoride, while the structures of complexes with benzene and bromide are presented in Supplementary Material, Fig. S13. In the case of complexes formed with aromatic guests (Fig. 6a and Fig. S13a), the conformation of dyad **2** does not suffer significant changes upon complex formation. Thus, the values of the interplanar angle defined between NAPIM and DANS moieties ([naphthalimide]N−NSO_2−C]) remain practically without change, *i.e.*, free dyad has an angle of 90.1°, while dyad **2**-benzene complex has 91.5° and for dyad **2**-naphthalene is 89.4°.

In the case of benzene, weak aryl C−H … π hydrogen bonds are formed between the DANS hydrogen atoms and the benzene ring. The bonding distance is 2.97 Å which are in the range of the values reported for this kind of interactions [21]. In the other hand; naphthalene interacts with both NAPIM and DANS chromophores in a face to edge fashion with distances of [naphthalimide]C−H … π (centroid) 2.78 Å and [dansyl amide]C−H … π (centroid) 4.57 Å. This finding agrees with results obtained in the ^{1}H NMR experiments and provide evidence of formation of aryl C−H … π interactions.

For anionic guests (Fig. 6b and Fig. S13b), is important to consider that TBA salts used in this study remain undissociated in solution due to the low dielectric permittivity of $CHCl_3$ [20]. Thus, we calculated the structure of the complexes considering that halide anions are TBA^+X^- ion pairs.

The anion-TBA ionic pairs are located close to the NAPIM moiety and are bonded by aryl C−H … anion interactions [21]. The shortest distances were observed between H_a and F^- (distance C−H···F^-: 2.3 Å) or Br^- (distance C−H···Br^-:2.85 Å) which agrees with the NMR data, *i.e.,* H_a signals shift to low field because of the subtraction of electronic density by the halide anion. The same effect has been reported for a bisarylethynyl urea receptor [22].

4. Conclusions

With the use of different spectroscopic techniques, we demonstrated that dyad **2** interact with electron-rich guests through aryl C−H … anion and aryl C−H … π interactions with binding constants in the range of 6×10^3 to 8×10^3 M^{-1} in $CHCl_3$. The affinity constants measured in this work are in the same order that those reported for other receptors and showed that compounds built as dyad **2** with two electron deficient moieties are versatile receptors able to interact with anions. Selecting the appropriate solvent it is possible to promote the partial dissociation of ionic pairs that can be augmented in the presence of electron-deficient receptors through aryl C−H … anion interactions.

Acknowledgment

This work was supported by CONACYT − México, project CB2010/158098 and RTQS project 281251. The authors thank LANEM laboratory for the use of NMR spectrometers.

Appendix A. Supplementary data

Supplementary data to this article can be found online at https://doi.org/10.1016/j.saa.2019.117553.

References

[1] S. Abad, M. Kluciar, M.A. Miranda, U. Pischel, Proton-induced fluorescence switching in novel Naphthalimide−Dansylamide dyads, J. Org. Chem. 70 (2005) 10565−10568, https://doi.org/10.1021/jo0512195.
[2] B.H. Shankar, D. Ramaiah, Dansyl—naphthalimide dyads as molecular probes: effect of spacer group on metal ion binding properties, J. Phys. Chem. B 115 (2011) 13292−13299, https://doi.org/10.1021/jp207895y.
[3] V.S. Jisha, A.J. Thomas, D. Ramaiah, Fluorescence ratiometric selective recognition of Cu2+ ions by Dansyl−Naphthalimide dyads, J. Org. Chem. 74 (2009) 6667−6673, https://doi.org/10.1021/jo901164w.
[4] S.-J. Li, D.-Y. Zhou, Y. Li, H.-W. Liu, P. Wu, J. Ou-Yang, W.-L. Jiang, C.-Y. Li, Efficient two-photon fluorescent probe for imaging of nitric oxide during endoplasmic reticulum stress, ACS Sens. 3 (2018) 2311−2319, https://doi.org/10.1021/acssensors.8b00567.
[5] M.A. Landey-Álvarez, A. Ochoa-Terán, G. Pina-Luis, M. Martínez-Quiroz, M. Aguilar-Martínez, J. Elías-García, V. Miranda-Soto, J.-Z. Ramírez, L. Machi-Lara, V. Labastida-Galván, M. Ordoñez, Novel naphthalimide−aminobenzamide dyads as *OFF/ON* fluorescent supramolecular receptors in metal ion binding, Supramol. Chem. 28 (2016) 892−906, https://doi.org/10.1080/10610278.2016.1149180.
[6] Y. Zhou, J.F. Zhang, J. Yoon, Fluorescence and colorimetric chemosensors for fluoride-ion detection, Chem. Rev. 114 (2014) 5511−5571, https://doi.org/10.1021/cr400352m.
[7] M.Á. Claudio-Catalán, F. Medrano, H. Tlahuext, C. Godoy-Alcántar, Crystal structure of N,N′-bis[2-((benzyl){[5-(dimethylamino)naphthalen-1-yl]sulfonyl}amino)ethyl]naphthalene-1,8:4,5-tetracarboximide 1,2-dichlorobenzene trisolvate, Acta Crystallogr. 72 (2016) 1503−1508, https://doi.org/10.1107/S2056989016015188.
[8] O.V. Dolomanov, L.J. Bourhis, R.J. Gildea, J.a.K. Howard, H. Puschmann, OLEX2: a complete structure solution, refinement and analysis program, J. Appl. Crystallogr. 42 (2009) 339−341, https://doi.org/10.1107/S0021889808042726.
[9] G.M. Sheldrick, Crystal structure refinement with SHELXL, Acta Crystallogr. C 71 (2015) 3−8, https://doi.org/10.1107/S2053229614024218.
[10] K. Brandenburg, DIAMOND, University of Bonn, Germany, 1997.
[11] P.J. Stephens, F.J. Devlin, C.F. Chabalowski, M.J. Frisch, Ab initio calculation of vibrational absorption and circular dichroism spectra using density functional force fields, J. Phys. Chem. 98 (1994) 11623−11627, https://doi.org/10.1021/j100096a001.
[12] Gaussian 09, Revision A.02, M. J. Frisch, G. W. Trucks, H. B. Schlegel, G. E. Scuseria, M. A. Robb, J. R. Cheeseman, G. Scalmani, V. Barone, G. A. Petersson, H. Nakatsuji, X. Li, M. Caricato, A. Marenich, J. Bloino, B. G. Janesko, R. Gomperts, B. Mennucci, H. P. Hratchian, J. V. Ortiz, A. F. Izmaylov, J. L. Sonnenberg, D. Williams-Young, F. Ding, F. Lipparini, F. Egidi, J. Goings, B. Peng, A. Petrone, T. Henderson, D. Ranasinghe, V. G. Zakrzewski, J. Gao, N. Rega, G. Zheng, W. Liang, M. Hada, M. Ehara, K. Toyota, R. Fukuda, J. Hasegawa, M. Ishida, T. Nakajima, Y. Honda, O. Kitao, H. Nakai, T. Vreven, K. Throssell, J. A. Montgomery, Jr, J. E. Peralta, F. Ogliaro, M. Bearpark, J. J. Heyd, E. Brothers, K. N. Kudin, V. N. Staroverov, T. Keith, R. Kobayashi, J. Normand, K. Raghavachari, A. Rendell, J. C. Burant, S. S. Iyengar, J. Tomasi, M. Cossi, J. M. Millam, M. Klene, C. Adamo, R. Cammi, J. W. Ochterski, R. L. Martin, K. Morokuma, O. Farkas, J. B. Foresman, and D. J. Fox, Gaussian, Inc., Wallingford CT, 2016.
[13] S. Miertuš, E. Scrocco, J. Tomasi, Electrostatic interaction of a solute with a continuum. A direct utilizaion of AB initio molecular potentials for the prevision of solvent effects, Chem. Phys. 55 (1981) 117−129, https://doi.org/10.1016/0301-0104(81)85090-2.
[14] G.R. Desiraju, T. Steiner, The Weak Hydrogen Bond: in Structural Chemistry and Biology, Oxford University Press, 2001.
[15] M.S. Alexiou, V. Tychopoulos, S. Ghorbanian, J.H.P. Tyman, R.G. Brown, P.I. Brittain, The UV−visible absorption and fluorescence of some substituted 1,8-naphthalimides and naphthalic anhydrides, J. Chem. Soc., Perkin Trans. 2 (1990) 837−842, https://doi.org/10.1039/P29900000837.
[16] P. Ceroni, I. Laghi, M. Maestri, V. Balzani, S. Gestermann, M. Gorka, F. Vögtle, Photochemical, photophysical and electrochemical properties of six dansyl-based dyadsDedicated to Professor Alex von Zelewsky on the occasion of his 65th birthday, New J. Chem. 26 (2002) 66−75, https://doi.org/10.1039/b105497j.
[17] H.J. Schneider, A. Yatsimirsky, Principles and Methods in Supramolecular Chemistry, John Wiley & Sons, England, 2000.
[18] M.S. Cubberley, B.L. Iverson, 1H NMR investigation of solvent effects in aromatic stacking interactions, J. Am. Chem. Soc. 123 (2001) 7560−7563, https://doi.org/10.1021/ja015817m.
[19] M.B. Inoue, F. Medrano, M. Inoue, Q. Fernando, Amide-based [12]-, [12.12]- and [12.12.12.12]paracyclophanes: non-planarity of amide and phenyl groups in the [12]cyclophane, J. Chem. Soc., Perkin Trans. 2 (1998) 2275−2280, https://doi.org/10.1039/A803417F.
[20] K. Iseda, K. Kakado, K. Sada, Direct detection of the ion pair to free ions transformation upon complexarion with an ion receptor in non-polar solvents by using conductometry, Chem. Open 7 (2018) 269−274, https://doi.org/10.1002/open.201800014.
[21] M. Nishio, The CH/π hydrogen bond in chemistry. Conformation, supramolecules, optical resolution and interactions involving carbohydrates, Phys. Chem. Chem. Phys. 13 (2011) 13873−13900, https://doi.org/10.1039/C1CP20404A.
[22] B.W. Tresca, L.N. Zakharov, C.N. Carroll, D.W. Johnson, M.M. Haley, Aryl C—H···Cl− hydrogen bonding in a fluorescent anion sensor, Chem. Commun. 49 (2013) 7240−7242, https://doi.org/10.1039/c3cc44574g.